Simulation of Remote Sensing Reflectance and Ocean Color Algorithms for High Resolution Ocean Sensor

Yu-Hwan Ahn, P. Shanmugam and Jeong-Eon Moon

Korea Ocean Research and Development Institute, Seoul, 425-600, Korea

yhahn@kordi.re.kr

Abstract: Retrieval of ocean color information from Multi-spectral Camera (MSC) on KOMPSAT-2 was investigated to study and characterize small-scale biophysical features in the coastal oceans. Prior to the derivation of such information from space-acquired ocean color imageries, the atmospheric effects largely from path and the air-sea interface should be removed from the total signal recorded at the top of the atmosphere (T_{TOA}). In this study, the "path-extraction" is introduced and demonstrated on the TM and SeaWiFS imageries of highly turbid coastal waters of Korea. The algorithms for retrieval of ocean color information were explored from the remote reflectance (R_{rs}) in the visible wavebands of MSC. The determination of coefficient (R^2) for log-transformed data [<chl> N = 500] was 0.90. Similarly, the R^2 value for log-transformed data [<SS> N = 500] was found to be 0.93.

Keywords: Ocean color, path-radiance, Multispectral Camera.

1. Introduction

The color of the ocean measured from space, which can be determined by the reflectance ratio of upwelling (E_u) to downwelling irradiance (E_d) just beneath the surface, provides information on the abundance of the coastal and open oceanic water constituents such as phytoplankton, dissolved organic matter and suspended sediment particulate materials. The launch of CZCS on Nimbus-7 satellite in 1978 has made a significant contribution to the ocean color community to study the spatial and temporal evolution of phytoplankton distribution in the open oceanic waters, characterizing the highly dynamic features such as eddies, meanders and variability of ocean circulation patterns at local and regional scales (Barale and Trees 1987). The end of CZCS in 1986 has resulted several other ocean color radiometers with improved spatial and spectral characteristics. Along with these instruments, the high-resolution sensors specifically developed for land applications are also used for deriving ocean parameters at high spatial resolution (Doxaran *et al*. 2002). Along this line, the Multi-spectral Camera on Kompsat-2 satellite is expected to make significant contributions to the enhanced understanding of the coastal oceans. In the present study, we develop a methodology that would consist of an atmospheric correction method and ocean color algorithms for MSC. The methodology presented here can also be extended to other ocean color sensor to enable accurate estimates of chlorophyll and suspended sediment concentrations in the coastal oceans.

2. Atmospheric correction of ocean color imageries

It is well known that the radiance measured at the top of the atmosphere is primarily composed of the atmospheric scattered radiance due to air molecules and aerosols, air-sea interface reflected radiance and the transmitted water-leaving radiance. It is, therefore, very essential to remove the atmospheric and ocean surface effects before retrieving ocean color information from space-acquired imageries. In the present study, an attempt is made to correct the atmospheric and air-sea interface effects in the visible and near infrared domains of ocean color imageries. A simple method is presented to extract the path radiance (L_{atm} +$L_{a\text{-}s}$) from the total radiance (L_{TOA} = L_{atm}+$L_{a\text{-}s}$+L_w) recorded at the top of the atmosphere (L_{TOA}), hereafter referred to as "Path-Extraction". The main assumption behind path-extraction is that the least signal of a few pixels of a given image is attributed to the path-radiance of the atmosphere and the air-sea interface. We test this method on the TM and SeaWiFS imageries of highly turbid coastal waters of Korea. The spectral form of the path-extracted water-leaving radiance is then compared with water-leaving radiance spectra of the standard SeaWiFS atmospheric correction algorithm. Fig 1a represents the total radiance, path radiance and the path-extracted water-leaving radiance in SeaWiFS wavebands. It is seen that the path-extracted water-leaving radiance progressively increases from blue to red wavebands and gradually decreases toward NIR wavebands (Fig. 1b). The water-leaving radiance retrieved from Level 1A SeaWiFS product using the standard atmospheric correction algorithm is shown in Fig 1c. It is clearly evident that the standard SeaWiFS algorithm leads to essentially underestimate the L_w values through out the shorter wave bands and produces large errors for extremely turbid coastal water [<SS> Conc. >100 (g/m^3)], which is not able to be distinguished from moderately turbid pixels. It is observed that *in situ* spectrum coincidently collected during SeaWiFS overpass (1998/10/21) in the southern coastal waters resembles the path-extracted water leaving radiance spectrum (Fig. 1d)). A small discrepancy between the *in situ* and path-extracted water-leaving radiance is due to the fact that the *in situ* spectrum was derived from a point measurement while the path-extracted water-leaving spectrum was based on pixel measurement (1.13×1.13km).

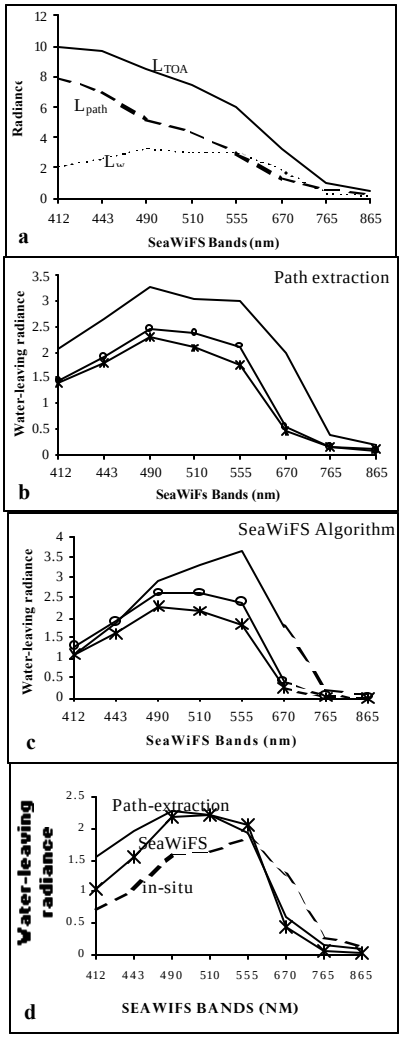

Figs. 1a-d: Results of atmospheric correction method

3. Derivation of Empirical Algorithms

A large number of remote reflectances were generated using Ahn's R_{rs} model (1999) and converted to the equivalent reflectances at three MSC bands. Figs 2a and b show the reflectance spectra with varying chlorophyll (0.74~30.2mg/m^3) and suspended sediment concentrations (9.2~88.7g/m^3). It is seen that the absorption by pigments is very significant in the blue and red wavebands while the scattering by organic particles is normally attributed to the green waveband (Ahn, 1990). Therefore, the decreased reflectance in the blue and increased reflectance in the green can be effectively adopted to derive an empirical algorithm by taking the ratio of these two wavebands. For estimating SS concentration, we relate only a single band reflectance (green) to the suspended sediment concentrations.

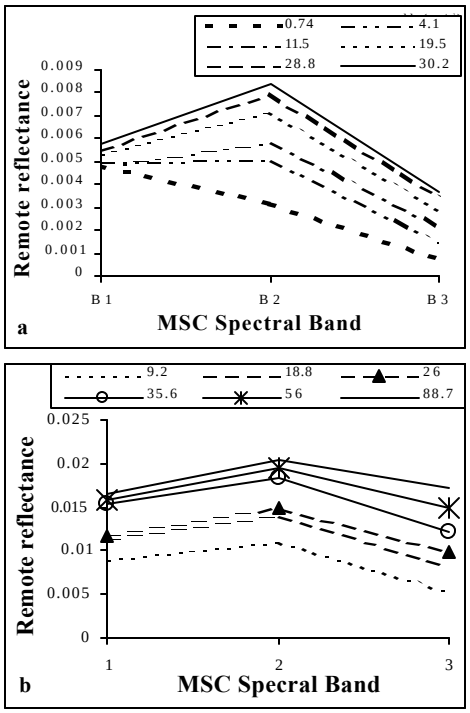

Figs. 2a & b: Remote sensing reflectance spectra for different *<chl>* concentrations and *<SS>* concentrations.

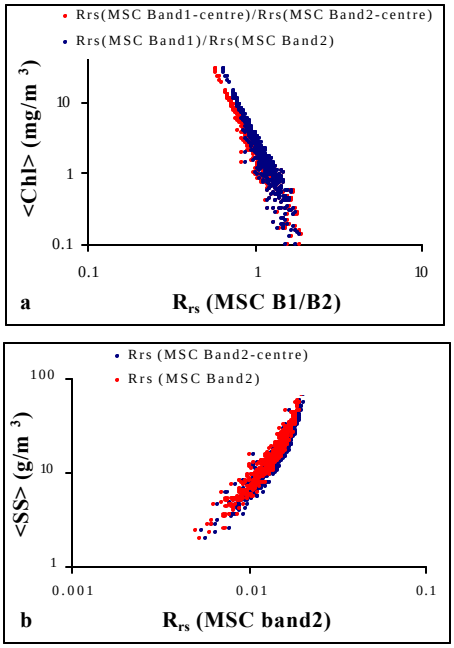

Fig. 3a. Relationship between the ratios of MSC band reflectances and *<chl>* concentrations. (b) Relationship between MSC green band reflectance and *<SS>* concentration.

Fig. 3a shows the relationship between the spectral ratios of remote reflectances, [R_{rs}(MSC Band1)/ R_{rs}(MSC Band2)] and [R_{rs}(MSC Band1-centre)/R_{rs}(MSC Band2-centre)] and chlorophyll concentrations [$<chl>$ (mg/m^3)]. It is observed that there is not much difference between the values of the spectral ratios of the broad and center wavebands. The empirical equation for <chl> is expressed as follows

$$<chl>[mg/m^3]=2.93x^{-4.89}$$

The squared correlation coefficient for these log-transformed data is R^2 = 0.90. Similarly, an empirical formula for center waveband relationship is expressed as

$$<chl>[mg/m^3]=2.37x^{-4.25}$$

with R^2= 0.91. Where x defines the spectral ratios of broad and centre wavebands. For each case, the total

number of observations, $N = 500$. The power equation was used to relate R_{rs} ratio to the chlorophyll concentration because of the relative ease of derivation of model parameters using a simple linear regression of log-transformed data (Smith and Baker, 1982). Similarly, <*SS*> algorithms were derived from the relationships, [R_{rs}(MSC Band2)] and [R_{rs}(MSC Band2-centre)] verses SS concentrations, and examined (Fig. 3b).

$$<\text{SS}> (\text{g/m}^3) = 0.89e^{205.7x}, [R^2 = 0.92]$$

$$<\text{SS}> (\text{g/m}^3) = 0.81e^{202.4x}, [R^2 = 0.91]$$

where x is the green band reflectance. For estimating SS concentration, the broadband is seemingly better than the center band if we consider the correlation coefficient values $R^2 = 0.92$. The relationships made between the remote reflectances and <*chl*> and <*SS*> have some similarities with the existing NASA OC2and OC4 algorithms, since the center waveband does not have much differences with the broadband relationship.

4. Conclusion

Potential use of path extraction and ocean color algorithms were demonstrated in the previous sections. Path-extraction was found to be more efficient method to remove the atmospheric effects from the imageries of the Landsat-TM and SeaWiFS. Since the differences between the values of the spectral ratios of remote reflectances at the broad and center wavebands are very small, the broadband algorithms presented here are expected to yield accurate information about the chlorophyll and suspended sediment concentrations in the coastal oceans. These information are not accurate with currently existing ocean color sensors of having poor spatial resolution, which may have sub-pixel variability, especially in the coastal oceans. In this study, we excluded the use of the band ratio algorithm for estimating SS concentration because the influence of DOM absorption is significant in the blue waveband (Ahn, 2000 and Ahn *et al*., 2001).

References

[1] Ahn, Y.H, 1990. Optical properties of biogeneous and mineral particles present in the ocean. Application: Inversion of reflectance. *Ph.D thesis*, Paris-VI University, France.

[2] Ahn, Y.H, 1999. Development of an inverse model from ocean reflectance. *Marine Technology Society Journal*, 33, 69-80.

[3] Ahn, Y.H, 2000. Development of remote sensing reflectance and water leaving radiance models for ocean color remote sensing technique. *Journal of the Korean Society of Remote Sensing*, 16, 240-260.

[4] Ahn, Y.H., J.E. Moon and S. Gallegos, 2001. Development of suspended particulate matter algorithms for ocean color remote sensing. Korean Journal of Remote Sensing, 17, 285-295.

[5] Barale, V and C.C. Trees, 1987. Spatial variability of the ocean color field in CZCS imagery. *Advances in Space Research*, 7, 95-100.

[6] Doxaran, D., J.M. Froidefond., S. Lavender and P. Castaing, 2002. Spectral signature of highly turbid waters. Application with SPOT data to quantify suspended particulate matter concentrations. *Remote Sensing of Environment*, 81, 149-161.